JOURNAL OF COMPUTATIONAL PHYSICS 89, 1–30 (1990)

The Monte Carlo Flux Method

G. SCHAEFER AND P. HUI

Weber Research Institute, Polytechnic University, Farmingdale, New York 11735

Received December 20, 1988, revised June 16, 1989

A new computational method—*Monte Carlo flux method* (MCF)—is presented, which allows calculating electron distribution functions in weakly ionized gases of stationary molecules subjected to electric and magnetic fields. This method should be equally suited for calculating electron distribution functions in semiconductors. The method utilizes a modified Monte Carlo code to calculate transition probabilities for electrons between phase cells. Transport equations utilizing these transition probabilities are used to calculate steady state and transient distribution functions. Electron generation and depletion processes are easily incorporated. Numerical calculations of space independent electron distribution functions in nitrogen (N_2) are presented for both steady state and transient conditions, and compared with results obtained with *conventional Monte Carlo* (CMC) calculations. The major advantages of the new method are discussed.

I. INTRODUCTION

One of the persistent problems of crucial importance in collisional plasmas is obtaining knowledge of the space time dependent velocity distribution function, $f(\mathbf{r}, \mathbf{v}, t)$, for the changed particles. At this time there are no means available to measure space and time dependent electron velocity distribution functions directly. Therefore, they have to be evaluated from measurable quantities such as rates and transport coefficients. To do this we depend on models which allow calculating distrubution functions and relating the distribution functions to such experimentally available data.

Calculations of the electron distribution functions in collisional plasmas are based on numerical solutions of the Boltzmann equation utilizing a set of experimentally obtained cross sections which should be as complete as possible. The most common approaches are Boltzmann analysis and Monte Carlo technique. In the first approach the distribution functions are expanded, usually into a series of Legendre polynomials. In this way the Boltzmann partial differential equation is converted into a set of coupled ordinary differential equations and each angular moment of the distribution function can be determined under certain approximations. For practical reasons one has to limit the number of terms and often only two terms are considered. For highly anisotropic distributions (high values of E/N,

0021-9991/90 $3.00

where E is the electric field intensity and N is the gas density) or in cases where the wings of the distribution (usually the part of the distribution which has the higher anisotropy—see Section IV) are of major interest one has to increase the number of terms. It was shown by Allis [1] that under some conditions the calculated distribution function can become negative and that in a certain energy range the magnitude of a higher order angular moment can be greater than a lower one; in other words, convergence of Boltzmann analysis is not guaranteed.

In the *conventional Monte Carlo* (CMC) technique the electron trajectories are calculated and collisions of electrons with molecules in the gas are simulated by Poisson stochastic processes, and the states of electrons are sampled at certain time intervals. The statistical information can be obtained after evaluating a sufficiently large number of electrons or, for steady state calculations, after following one or a few electrons for a long enough period of time. Since the number of electrons sampled in a phase cell is the product of the function value at this phase cell, the volume of the phase cell, and the number of electrons studied, high resolution and small CPU time are contradictory to each other. This problem is especially serious in the wings of the distribution functions where the function value is inherently small.

In order to increase the resolution in cases where the electrons in the wings of the distribution do not strongly interact with the rest of the electrons, methods have been used to renormalize the distribution function with changing weight factors during the calculation [2–4] or to recalculate the wing in a separate calculation [5]. In many other cases, however, these approaches are not feasible.

Similar problems can occur in CMC calculations of electron distributions in semiconductors. Weighting procedures have been used to extend hot electron distributions to rarely occupied ranges [6]. Also in multivalley semiconductors at low electric fields only a small fraction of electrons populate the upper valley. To obtain an accurate presentation of electrons in this valley it is necessary to increase the number of electrons used in a CMC simulation [7].

As an alternative we proposed the *Monte Carlo flux* (MCF) method [8–10]. To increase the resolution of the calculation also in the wings of the distribution function, we have to be able to adjust the number of test particles, going into and out of a phase cell of any desired range of the phase space, independently of the final value of the distribution function at this phase cell. Quantities which can be calculated based on this condition are transition probabilities (or particle flux) for transitions between different phase cells. The final distribution function can be calculated from these transition probabilities.

In Section I we addressed the problems associated with both the Boltzmann analysis and the Monte Carlo technique and explained the main idea of the MCF method. The physical basis and mathematical formulation of the MCF method will be presented in Section II for cases in which electron generation and depletion processes can be neglected. In Section III we will discuss how to incorporate generation and depletion mechanisms. Section IV presents numerical results obtained using the MCF method and, for comparison, results obtained using the CMC technique.

II. The Mathematical Formalism of the Monte Carlo Flux Method

In this section we describe the MCF method for conditions under which electron generation and depletion processes can be neglected and no density gradients occur. Since the CMC technique is well known, we will emphasize the features of the MCF method and mention some similarities between the two methods.

The statistical behaviors of electrons in gases subjected to an electric field can be described by the distribution function, $f(\mathbf{r}, \mathbf{v}, t)$, in the phase space $(\mathbf{r}, \mathbf{v})$. In the homogeneous case we only need to consider the velocity distribution, $f(\mathbf{v}, t)$. If the direction of the electric field does not change, this problem has axial symmetry with respect to the direction of the electric field (negative z-direction) and the velocity distribution reduces to $f(v, \mu, t)$ with $\mu = v_z/v$. In this case the $\mathbf{v}$-space is only two-dimensional, however; the MCF method can also be used for calculating three-dimensional velocity distribution functions such as in $\mathbf{E} \times \mathbf{B}$ fields.

The knowledge of $f(\mathbf{v}, t)$ can be obtained by either solving the Boltzmann equation or performing a CMC simulation. As mentioned in Section I both methods have some limitations. We will not further discuss the convergence problem of Boltzmann analysis, which has been discussed in detail by Allis [1]. On the other hand, the discussion of some of the problems related to the CMC is helpful in understanding the MCF method.

A. *The Conventional Monte Carlo Technique*

For the CMC technique the phase space is first discretized. The way of discretization and the size of the phase cells depend on the specific problem. In our example ($\mathbf{E}$ = constant in negative z-direction), the phase is only two-dimensional, (v, μ). The motions of electrons in the phase space are calculated by following their trajectories and simulating their collisions with background molecules via random variables. At the same time the states of electrons are sampled and stored. After a predetermined number of samples the statistical information of the electrons in gases under the influence of the external electric field is obtained. The CMC technique is a bookkeeping procedure, which is not difficult to implement.

As mentioned before, the CMC technique has severe disadvantages such as the significant amount of computer time needed and the low resolution in the wings of the distribution function. We know that the statistical error of the simulation is inversely proportional to the number of samplings. The number of electrons sampled in a phase cell is determined by the value of the distribution function at the cell, the volume of the cell, and the total number of electrons studied. Let us, for example, assume that we have discretized the velocity range of interest into 10^2 intervals and that we have sampled 10^6 electron states. In the high velocity wings of the distributions the function values are very small, and the ratio to the maximum value can be in the order of 10^{-4} and lower. This corresponds to only one or a few electrons sampled per velocity interval of the wing. In order to reduce the statistical error in this velocity range we have to increase either the total number

of counts which means to increase the CPU time or the size of the phase cells which means to decrease the velocity resolution of the simulation.

The problems associated with the CMC technique come from the fact that the number of electrons sampled in a phase cell is directly proportional to the value of the distribution function. In order to reduce the statistical error in the wings of the distributions we have to be able to increase the number of test electrons appearing in the high energy range in such a way that we get approximately the same resolution over the full distribution. With this requirement in mind, we will develop mathematical formulation of the MCF method.

B. *The Monte Carlo Flux Method*

For the MCF method the phase space is again first discretized. Just as in the CMC technique this requires some prior knowledge of the extension of the relevant phase space for a given boundary condition. In this method we treat each phase cell as a state which electrons can occupy with a certain probability. The state of electrons is then described by specifying the relative probability of finding electrons in any such state. Instead of using the relative probability we can also use the density of electrons in phase space to describe the state of electrons. The only difference between these quantities is the normalization constant, which is the electron density in the real space, n_e. Depending on the specific situations we will use both terminologies in the later text.

The statistical ensemble motion of the electrons in the phase space is then described by the transition probabilities (or particle flux) of electrons for transitions between different phase cells within a time step, t_s. The definition of the transition probability, $p_{ij}(t_s)$, for a given field configuration is the probability for an electron to appear in the phase cell j at the time t_s under the condition that it was in phase cell i at the time $t=0$.

In the Monte Carlo flux method we use a modified Monte Carlo code to calculate these transition probabilities. It should be mentioned here that any other method used to solve the Boltzmann equation can also be utilized to calculate these transition probabilities. For example, equivalent transition probability rates in energy space have been calculated based on the two-term expansion [11]. By using a modified Monte Carlo simulation code, as discussed below, we can calculate these transition probabilities for a given value of E/N as

$$p_{ij}(t_s) = N_{ij}(t_s)/N_i(0), \tag{1}$$

where $N_{ij}(t_s)$ is the number of electrons observed in the phase cell j after the sampling time, t_s, and $N_i(0)$ is the number of electrons introduced into the phase cell i at $t=0$. The number of electrons introduced into phase cell i at $t=0$, $N_i(0)$, which determines the resolution of the calculation, can be adjusted independently of the function value of the distribution at the phase cell i. For a balanced resolution over the full distribution one would typically select $N_i(0)$ to be constant (independent of i).

Since at this time no electron generation and depletion processes are considered, the total number of electrons introduced into phase cell i at time $t=0$ can be expressed as:

$$N_i(0)=\sum_j N_{ij}(t_s). \tag{2}$$

Taking the summation of Eq. (1) over subscript j and using Eq. (2), we obtain

$$\sum_j p_{ij}(t_s)=1 \tag{3}$$

which is the equation for the conservation of the number of electrons. Equation (3) is not exact since Eq. (1) contains a statistical error, which can be reduced by increasing $N_i(0)$ and decreasing the size of the phase cell; however, conservation of particles is numerically guaranteed in the MCF method. The error in calculating the transition probabilities, $p_{ij}(t_s)$, will, of course, affect the accuracy of the distribution function.

Let us denote the density of electrons in phase cell i by n_i ($i=1, 2, ...$). Thus the two states of electrons at the time $t=0$ and $t=t_s$ are specified by state vectors, $\mathbf{n}(0)$ and $\mathbf{n}(t_s)$, respectively, whose elements are

$$\mathbf{n}(0)=\{n_1(0), n_2(0), ...\}' \tag{4}$$

$$\mathbf{n}(t_s)=\{n_1(t_s), n_2(t_s), ...\}'. \tag{5}$$

The density of electrons appearing in phase cell j at the time $t=t_s$, $n_j(t_s)$, is connected to the densities at $t=0$ and the transition probabilities through the transport equation:

$$n_j(t_s)=\sum_i p_{ij}(t_s)\, n_i(0) \qquad (j=1, 2, ...). \tag{6}$$

Equation (6) can be written in the matrix form

$$\mathbf{n}(t_s)=\mathbf{P}'(t_s)\,\mathbf{n}(0); \tag{7}$$

here $\mathbf{P}(t_s)$ is the transition matrix, defined as

$$\mathbf{P}(t_s)=\{p_{ij}(t_s)\} \tag{8}$$

and $\mathbf{P}'(t_s)$ is the transposed matrix of $\mathbf{P}(t_s)$. The function of the transition matrix, $\mathbf{P}(t_s)$, is mapping the initial state vector, $\mathbf{n}(0)$, into $\mathbf{n}(t_s)$ after a time step, t_s.

For the transient case, we can simply update the distribution function by time steps with the length t_s using the transport Eq. (7). Obviously, the time step, t_s, is the resolution of this method with respect to time.

For the steady state case, as a special case of the transient one, where $\mathbf{n}(t_s) = \mathbf{n}(0) = \mathbf{n}$, we have

$$\mathbf{n} = \mathbf{P}'(t_s)\mathbf{n}. \tag{9}$$

Equation (9) is an eigenvalue problem. From Eq. (3) we can prove that its eigen equation

$$\det\{\mathbf{P}'(t_s) - \mathbf{I}\} = 0 \tag{10}$$

always holds [12]. This means that there exists at least one nontrivial solution $\mathbf{n}$ to Eq. (9). However, for our assumed physical system there is only one solution. Thus the distribution function for the steady state case is the normalized eigenvector of the matrix, $\mathbf{P}'(t_s)$, corresponding to the unit eigenvalue.

For the case in which no electron generation and depletion mechanisms are involved, the electron density, n_e, is not defined. Therefore, we can only determine the normalized distribution, $\mathbf{n}/n_e$. Generation and depletion mechanisms will be discussed in Section III.

The mathematical model used in the MCF method is the Markov chain [12]. Equation (7) shows that the past has no influence on the future if the present is specified. This imposes specific conditions on the selection of the time step, t_s, which controls the transition probabilities (or flux) of electrons going from one phase cell to another. The introduction of $N_i(0)$ test electrons into phase cell i at $t = 0$ has to be done in some random fashion equally distributed over the volume of the phase cell. The condition for a Markov chain is fulfilled only if those electrons which have moved within the time, t_s, into phase cell j are again distributed in a random manner. In this respect the influences of collisions and of the applied electric field are quite different. The collisions are simulated by random variables (for the free flight time, type of collisions, and scattering angle) and will, in general, fulfill this condition. The acceleration of electrons between two successive collisions in the electric field, however, is deterministic. The minimum time step, $(t_s)_{\min}$, is therefore defined by the condition that the velocity component in electric field direction, v_z, changes by an amount equivalent to the width of the phase cell in v-direction.

The major difference between the MCF method and the CMC technique is that in calculating the transition probabilities the electrons are not followed over a long period of time, but only over the sampling time, t_s. One important feature of the MCF method is that the number of electrons introduced into any state can be chosen independent of the final value of the distribution function since the transition probabilities are conditional. Because of this property we can introduce as many electrons into any phase cell in the wings as those into the low energy range. This property of the MCF method implies that the resolution of the calculation of the full distribution function will be improved and that the CPU time needed will be reduced.

For the steady state case we only had to calculate the eigenvector of the matrix

$\mathbf{P}'(t_s)$, which was obtained for a constant value of E/N, subject to the normalization condition. In the transient case, however, E/N changes with time and, as a consequence, the transition matrix in the transport Eq. (7) should also change with time. In a practical code one, therefore, has to provide a library of transition matrices for different values of E/N in the E/N range of interest, and time dependent calculations are approximated by a number of stepwise changes of E/N. E/N has to be kept constant for at least one time step, t_s.

In the following we will, therefore, restrict ourselves to the simplest case in which E/N is constant and the initial distribution is different from the one of the steady state case for this value of E/N. This condition is, for example, given in the case where the external electrical field jumps from one value to another at the time $t=0$. Under this assumption, the transition matrix is fixed for $t>0$ and the state vector of the electrons after any number of time steps, kt_s, can be evaluated according to the following equation:

$$\mathbf{n}(kt_s)=(\mathbf{P}'(t_s))^k\,\mathbf{n}(0), \qquad k\text{: integer.} \tag{11}$$

In order to understand how the initial state vector relaxes to the final one, it is necessary to look at the spectrum of the transition matrix. Assuming that the eigenvalues and the corresponding eigenvectors of the matrix $\mathbf{P}'(t_s)$ are λ_i and $\mathbf{n}_i$ ($i=1, 2, ...$), respectively, we can expand the state vector at the time $t=kt_s$ (k: integer) as

$$\mathbf{n}(kt_s)=\sum_i c_i\lambda_i^k\mathbf{n}_i \tag{12}$$

where the expansion coefficients c_i ($i=1, 2, ...$) depend on the initial state vector, $\mathbf{n}(0)$, and the eigenvectors $\mathbf{n}_i$ ($i=1, 2, 3, ...$).

We already know that the maximum eigenvalue of the transition matrix, λ_1, is one because of Eq. (3) [12]. The further study reveals that the expansion coefficient c_1 is one. Thus Eq. (12) can be written as

$$\mathbf{n}(kt_s)=\mathbf{n}_1+\sum_i c_i\lambda_i^k\mathbf{n}_i. \tag{13}$$

As the time approaches infinity, only the first term on the right of Eq. (13) is left. The others disappear since the magnitudes of their eigenvalues are less than one. Thus, the first eigenvector of the matrix $\mathbf{P}(t_s)$, which was calculated for a constant value of E/N, is the steady state distribution at this value of E/N.

The higher order modes play an important role only during the transition phase. Without these modes the distribution function would not be continuous at time $t=0$. Since, at this moment, no electron generation and depletion processes are considered, the total number of electrons is conserved (see Eq. 3). Therefore the summation of the elements of any eigenvector is zero except for the one belonging to the unit eigenvalue.

III. Incorporation of Generation and Depletion of Electron

In the last section we have developed the MCF method for the case where no electrons are gained and lost. In this section we will discuss how to incorporate electron generation and depletion mechanisms into the MCF method. In general, a particular process can be incorporated either into the modified Monte Carlo code which is used to calculate the transition probabilities or into the transport Eq.(7). The optimum choice depends on the specific process considered.

1. *Ionization*

One step ionization is easily incorporated into the modified Monte Carlo code, considering the ionization cross section just as the one for any other collision process. The primary and the secondary electrons are followed until the end of the sampling time, t_s. Differential ionization cross section and the distribution of the partition of kinetic energy between primary and secondary electrons after ionizing collisions are available for some gases [13–15]. It is noted that, after the sampling time, t_s, electrons will appear in more than one state. As a result, the total number of electrons at the time t_s resulting from electrons in phase cell i is the total number of electrons introduced into phase cell i at the time $t=0$, $N_i(0)$, plus the number of electrons generated by ionization, $I_i(t_s)$. Now Eqs. (2) and (3) become

$$\sum_j N_{ij}(t_s) = N_i(0) + I_i(t_s) \tag{14}$$

$$\sum_j p_{ij}(t_s) > 1. \tag{15}$$

Equation (15) reflects the fact that the electron number increases with time due to ionization.

2. *Electron Attachment*

Only dissociative attachment will be discussed here, since it is the result of two body collisions. We assume that the density of the attaching molecules, n_a, is independent of the electron density. Attachment can be incorporated either into the modified Monte Carlo code or into the transport equation (7).

In the modified Monte Carlo code, we treat attachment in a way similar to ionization. The only difference is that the electron is removed whenever attachment occurs. Now Eq. (2) becomes

$$\sum_j N_{ij}(t_s) = N_i(0) - A_i(t_s), \tag{16}$$

where $N_i(0)$ is the number of electrons introduced into state i at the time $t=0$, $N_{ij}(t_s)$ is the number of transitions from phase cell i to j, and $A_i(t_s)$ is the number of attachment processes for electrons starting from state i within the sampling time,

t_s. Obviously, the summation of the transition probabilities of electrons leaving phase cell i will be less than unity, i.e.,

$$\sum_j p_{ij}(t_s) < 1. \tag{17}$$

Attachment can also be considered in the transport equation. In this approach we separate the transition matrix into two matrices. The first one, $\mathbf{P}_1(t_s)$, which is obtained by the modified Monte Carlo code, takes care of all processes in the gas except for attachment. The removed electrons due to the attachment will be included in the second matrix, $\mathbf{P}_2(t_s)$, as

$$(P_2)_{ij}(t_s) = \exp(-n_a \sigma_a v_i t_s)\, \delta_{ij}, \tag{18}$$

where

n_a: density of the attaching gas
σ_a: attachment cross section
v_i: mean speed within phase cell i
t_s: sampling time
δ_{ij}: kronecker delta function.

The total transition matrix is then approximated as the product of these two matrices. To conserve the symmetry property we define the total transition matrix as:

$$\mathbf{P}(t_s) = 0.5 * (\mathbf{P}_1(t_s)\, \mathbf{P}_2(t_s) + \mathbf{P}_2(t_s)\, \mathbf{P}_1(t_s)). \tag{19}$$

3. *Recombination*

The simplest case is dissociative recombination, since it is a two body collision. Similar to the case of attachment, we use two matrices to take care of recombination and the rest. Now the second matrix is

$$(P_2)_{ij}(t_s) = \exp(-n_+ \sigma_r v_i t_s)\delta_{ij}, \tag{20}$$

where

n_+: density of positive ion
σ_r: ionization cross section
v_i: mean speed within phase cell i
t_s: sampling time
δ_{ij}: kronecker delta function.

The total transition matrix is the same as given by Eq. (19) and the transport equation (7) is still valid. It should be noted that the matrix $\mathbf{P}_2(t_s)$ depends on the

ion density, n_+, which has to be calculated in a separate transport equation. For the special case of a recombination dominated discharge, we have

$$n_+ = n_e = \sum_i n_i \tag{21}$$

and $\mathbf{P}_2(t_s)$ is a function of the electron density, n_e. For the transient case the densities (n_+, n_e) and the matrix $\mathbf{P}_2(t_s)$ have to be updated after each time step t_s from Eqs. (20) and (21). This can be done easily, since matrix $\mathbf{P}_2$ is diagonal.

4. *External Source*

For external electron sources (X ray, UV radiation, particle beams, etc.) the electron generation rate does not depend on the electron density, n_e. It is therefore appropriate to add a source term, $\mathbf{n}_s$, to the transport equation (7). Now the generalized transport equation is

$$\mathbf{n}(t_s) = \mathbf{P}'(t_s)\,\mathbf{n}(0) + \mathbf{n}_s. \tag{22}$$

The source vector, $\mathbf{n}_s$, is given by

$$\mathbf{n}_{si} = S f_{in}(v_i)\,\partial \mathbf{v} t_s, \tag{23}$$

where

S: source function (number of electrons per unit volume and unit time)

$f_{in}(v)$: velocity distribution of the initial electrons produced by the external source

δv: volume of the phase cell

t_s: sampling time.

5. *Ionization and Recombination*

In the above we have shown how to incorporate individual electron generation and depletion processes into the MCF method. In this subsection we will give an example in which ionization and recombination are considered at the same time.

For all processes, except for recombination, we use the matrix $\mathbf{P}_1(t_s)$ to represent them, as discussed in the subsection III.1. Recombination is taken into account by the matrix $\mathbf{P}_2(t_s)$, whose elements are defined by Eq. (20). Then the total transition matrix can be approximated using Eq. (19).

For the steady state case, the number of electrons gained through ionization must be equal to the number of electrons lost through recombination. This requirement determines the electron density for the steady state, n_e, which can be obtained by solving the eigen equation (10). We now can easily obtain the normalized distribution $\mathbf{n}/n_e$ from Eq. (9). A steady state electron density, of course, only exists if electron generation and depletion processes are considered at the same time.

Since the matrix $\mathbf{P}_2(t_s)$ is diagonal, the calculation involved in solving the eigen equation (10) is not difficult. On the other hand, it is quite difficult to include electron generation and depletion processes in a CMC code, especially if the electron density changes significantly over time [3]. Therefore, the MCF method gives us a suitable way to study the influence of the electron generation and depletion mechanism on the distribution function.

IV. Numerical Results

In this section we present numerical results obtained using the MCF method and, for comparison, results obtained using the CMC method. All calculations were performed for the homogeneous case in nitrogen (N_2) at one atmosphere and room temperature ($N = 2.5 \times 10^{19}$ cm $^{-3}$) using the set of total and differential cross sections given by Phelps and Pitchford [16]. For the steady state case we compare the energy distributions, the angular distributions and the first six normalized Legendre coefficients at different values of E/N. As an example for the transient case we examine the response of the distribution function to a step function of E/N. The MCF code was used to calculate the time-dependent development of the distribution function. Since such calculations are too time-consuming with a CMC code, we performed such calculations only with low resolution to evaluate the relaxation of mean energy and drift velocity. In the MCF code we also incorporated ionization and recombination to calculate the steady state and time dependent

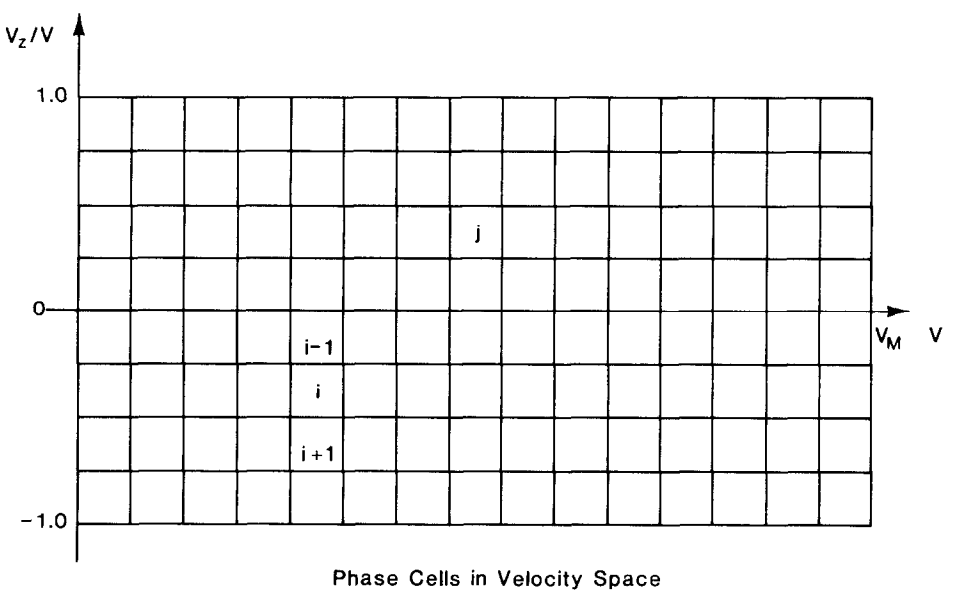

FIG. 1. Discretization of a two-dimensional velocity space.

electron density and to investigate the influence of the electron generation and depletion processes on the electron energy distribution.

In the formulation of the MCF method given in Sections II and III, the dimensions of the state vectors and the ranks of transition matrices are infinite. For numerical calculations we have to truncate the velocity to get finite rank matrices and finite order vectors. The preliminary knowledge of the required velocity range can be obtained either from experience or from a low resolution CMC simulation. Once the boundary of the velocity space is decided, we can discretize the two-dimensional velocity space (v, $\mu = v_z/v$) with a grid, as shown in Fig. 1. Each cell is a state which electrons occupy with certain probability. In our numerical calculations the velocity v was divided into 100 intervals and μ into 10. Thus the number of states is 1000 and size of the transition matrix is 1000×1000.

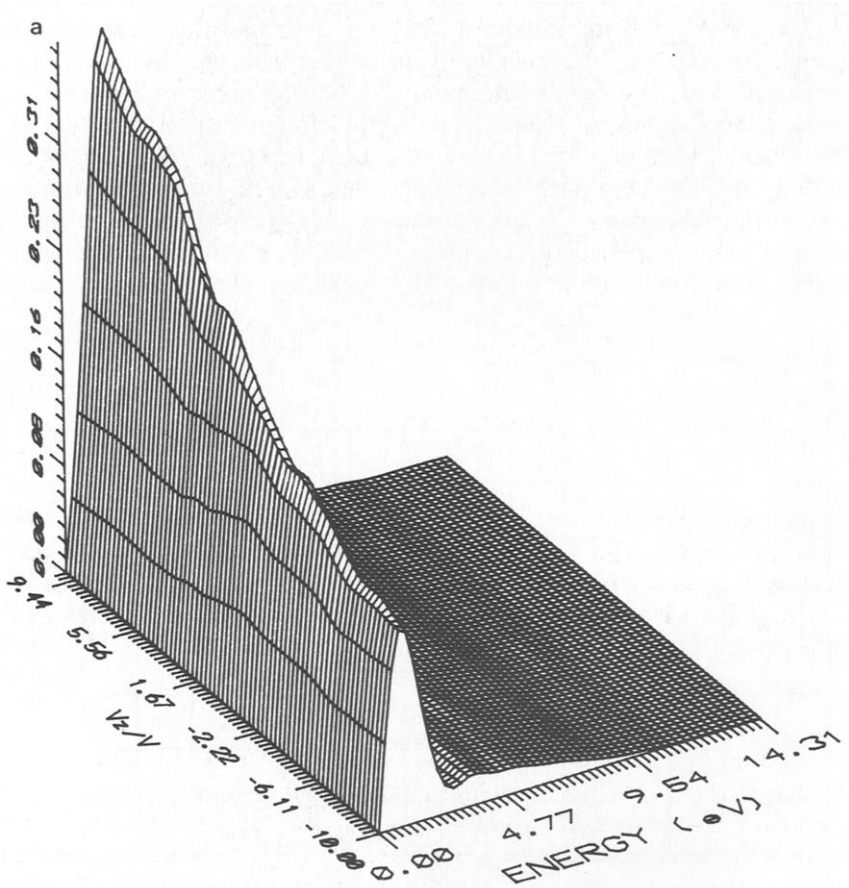

FIG. 2. Two-dimensional distribution functions $f(\varepsilon, \mu)$ obtained using the MCF method: (a) at $E/N = 100$ Td; (b) at $E/N = 300$ Td.

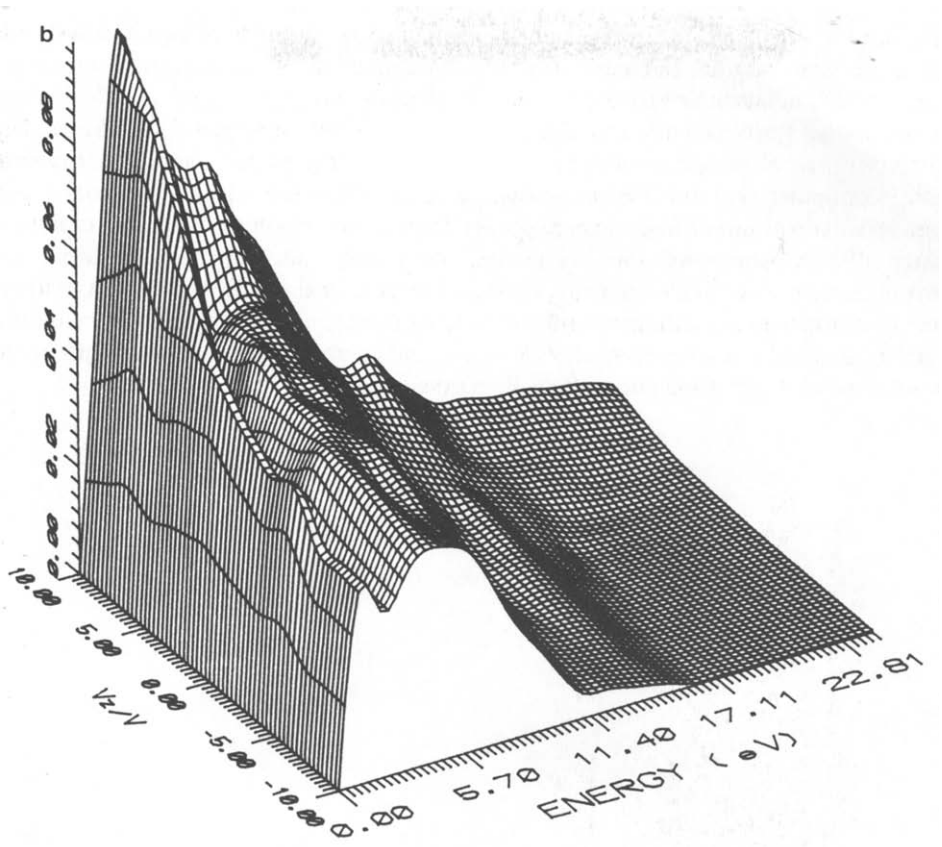

FIGURE 2 (*continued*)

For the calculations of the transition probabilities we introduced 1000 test electrons into each phase cell, uniformly distributed over the phase cell. This approach is a good approximation as long as the difference between the function value f_i in phase cell i and the function value in one of its direct neighbors j (see Fig. 1) is small compared to the function value itself, i.e.,

$$|f_i - f_j|/f_i \ll 1. \tag{24}$$

This condition is, for a sufficiently large dimension of the state vector, always fulfilled except for the phase cells with the lowest velocity. We, therefore, also tried to inject electrons into the low velocity phase cells according to a Maxwellian distribution; however, the numerical results showed that this was not necessary.

Electrons introduced into the phase cells with the highest values of the velocity can, within the time t_s, move beyond the boundary of the truncated part of the phase space. For the calculation of the transition probabilities we, therefore,

consider the phase cells with the highest velocity to be open in v-space, but only for the final state of the electron after the time t_s. This approximation preserves conservation of particle number.

As discussed in Section II the minimum sampling time, $(t_s)_{\min}$, is the time it takes an electron to be accelerated over the full width of the phase cell in v_z-direction. Larger sampling times give less statistical error of the steady state distrtibution but also less resolution of the time-dependence for the transient case. A transition matrix, $\mathbf{P}(t_s)$, which has been evaluated for short time steps, as required for calculating the relaxation of drift velocity or mean energy, can also be used to calculate transient conditions with long time constants such as the relaxation of the electron density. To save computer time one can reduce the number of time steps by a factor of k by using the transitive matrix:

$$\mathbf{P}_m(mt_s) = (\mathbf{P}(t_s))^m. \tag{25}$$

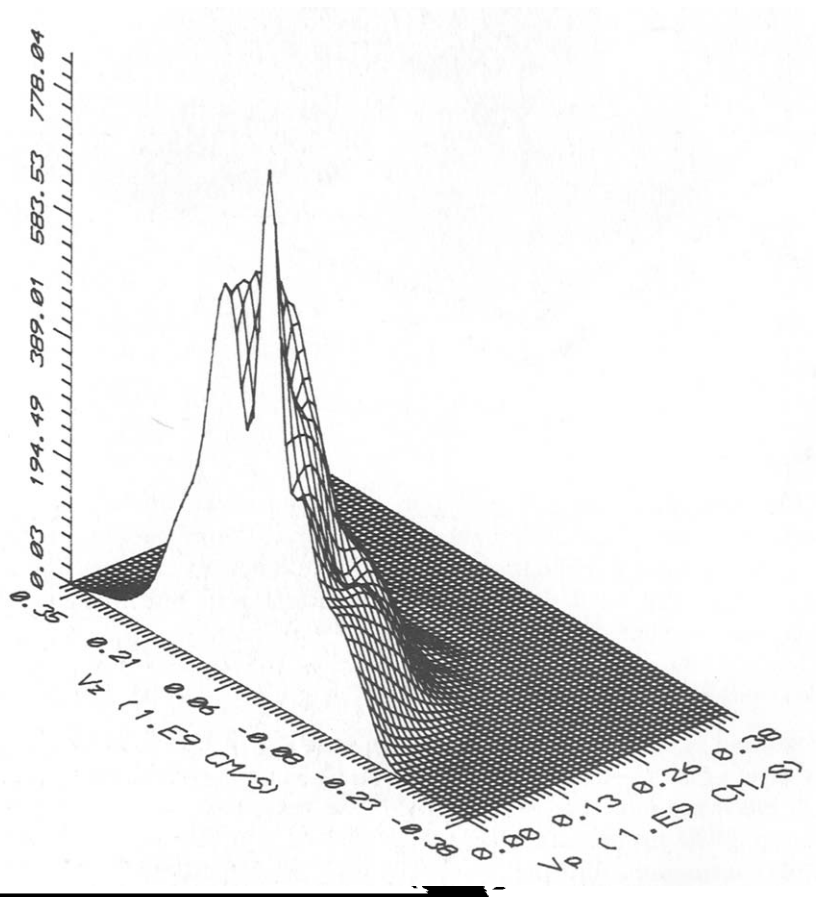

FIG. 3. Two-dimensional distribution function $f(v_p, v_z)$ obtained using the MCF method at $E/N = 300$ Td.

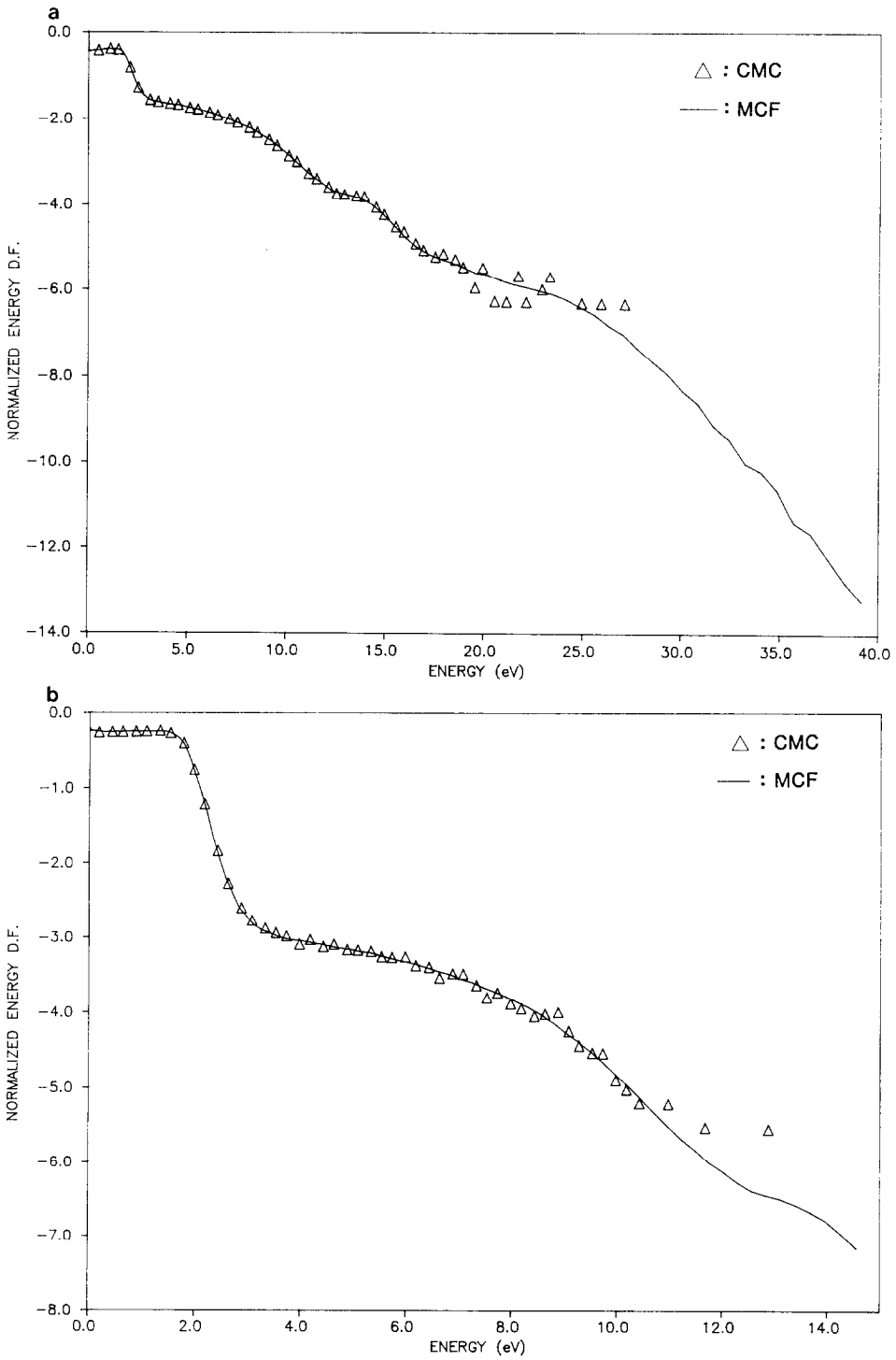

FIG. 4. Normalized electron energy distribution functions $f(\varepsilon)$: (a) at $E/N = 50$ Td; (b) at $E/N = 100$ Td (in logarithmic scale).

581/89/1-2

1. *Steady State Electron Velocity Distribution Functions*

All the calculations were originally performed in the velocity space. For the graphical presentation we converted the velocity-dependence into the energy-dependence. Figure 2 shows the two-dimensional distributions $f(\varepsilon, \mu)$ at $E/N = 100$ Td and $E/N = 300$ Td. In order to present a physical view of the two-dimensional distribution, we also show the velocity distribution at $E/N = 300$ Td in cylindrical coordinates (Fig. 3). These figures provide a clear picture of the electron distributions in the phase space and reveal some features typical for discharges in nitrogen (N_2) which will be discussed below.

All macroscopic quantities and one-dimensional distributions can be extracted from the two-dimensional distributions shown above. Integrating the two-dimensional function, $f(\varepsilon, \mu)$, over μ yields the energy distribution $f(\varepsilon)$. Figure 4 shows the normalized electron energy distribution functions at $E/N = 50$ Td and $E/N = 100$ Td obtained using both the MCF and the CMC method. The absolute resolution of the CMC simulation is limited to approximately 10^{-5} of its maximum value, corresponding to one count per velocity interval. This general limitation of the resolution in the wings of the distribution can only be improved by significantly increasing the computer time as discussed in Section II.A. The MCF method in

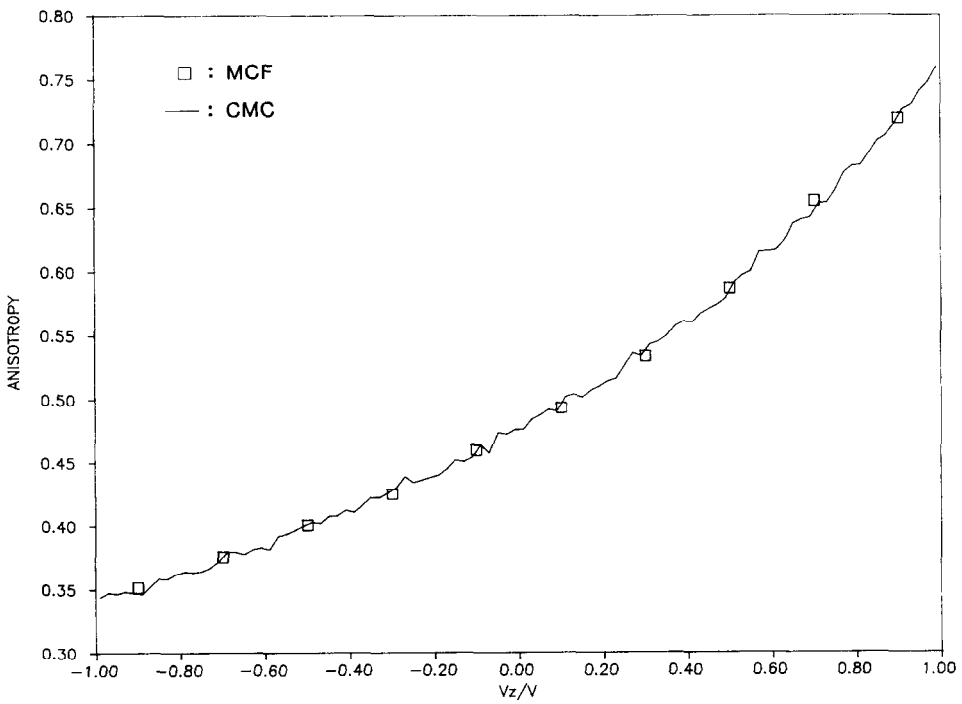

FIG. 5. Distributions of the anisotropy $f(\mu)$ obtained with both the CMC and MCF method.

comparison allows the calculation of the distribution function down to much lower values.

Through a similar procedure by integrating the two-dimensional function, $f(v, \mu)$, over the velocity, v, we obtain the distribution of the anisotropy $f(\mu)$. Figure 5 shows $f(\mu)$ at $E/N = 50$ Td and $E/N = 100$ Td. The results obtained using both the CMC and the MCF methods agree very well. The influence of E/N on the anisotropy is shown in Fig. 6. These curves, obtained using the MCF method, demonstrate the drastic increase of the anisotropy with increasing E/N.

It is obvious that, for specific values of E/N, the anisotropy of the distribution function is different in different energy ranges as can be seen, for example, from Fig. 2. For an easier interpretation of these results it may be advantageous to comprise the electrons into groups. For nitrogen (N_2) the energy dependence of the cross sections suggests consideration of three electron groups. N_2 has a large cross section for vibrational excitation with a maximum at approximately 2 eV which causes a minimum in the energy distribution function at this energy (see Fig. 2b) The electron group from 0 to 2 eV is, therefore, dominated by elastic collisions and vibrational excitation. Once electrons have passed the region of the high cross section for vibrational excitation they may only encounter elastic collisions until

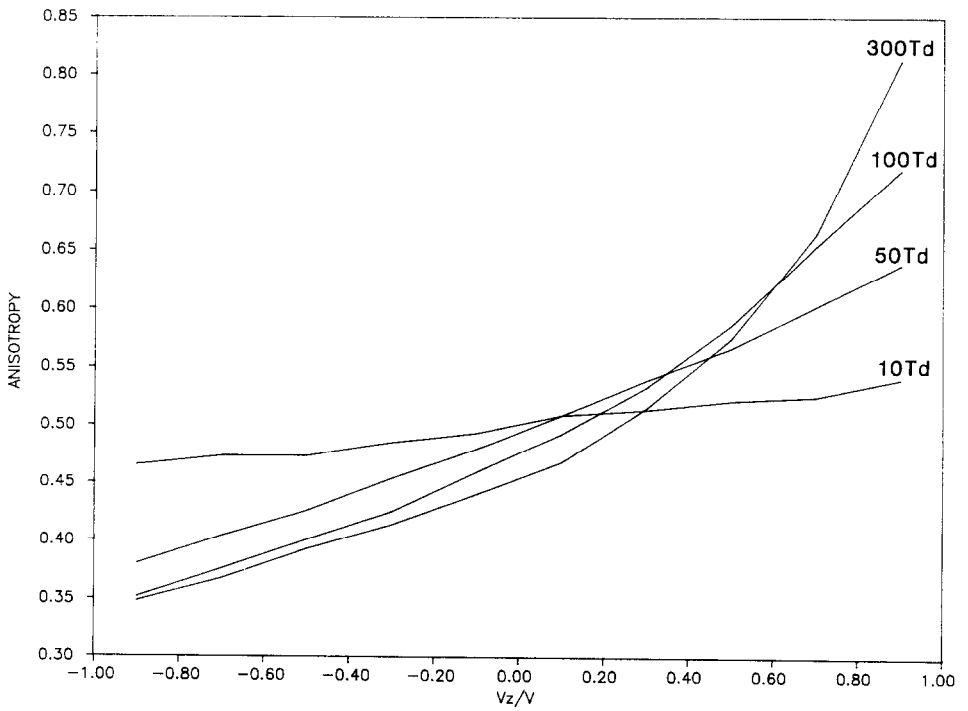

FIG. 6. Distributions of the anisotropy $f(\mu)$ at different values of E/N obtained using the MCF method.

they reach an energy of approximately 8 eV, where the region of electronic excitation starts. This energy region is also characterized by a significantly decreased value of the distribution function. The electrons in the energy region from 2 to 8 eV are, therefore, expected to be partially ballistic. Above 8 eV the distribution function is dominated by a large number of inelastic collision processes. Figure 7 shows the anisotropy for these three electron groups at $E/N = 100$ Td, demonstrating the existence of the highest anisotropy for the electron group from 2 to 8 eV.

2. *Comparison of the First Six Legendre Coefficients*

Usually, it is difficult to compare two-dimensional functions directly. One way is to expand two-dimensional functions into a series of given polynomials. For a comparison of the two-dimensional distributions $f(\varepsilon, \mu)$, calculated with both the MCF method and the CMC method, we evaluated the first six Legendre coefficients by using the Legendre transform. The results at $E/N = 300$ Td are shown in Fig. 8. The zeroth angular moment determines the mean value of energy and the first one determines the drift velocity. For these two moments the agreement between the MCF and the CMC method is very good. The agreement becomes worse for higher order moments. The first four normalized Legendre coefficients obtained using the

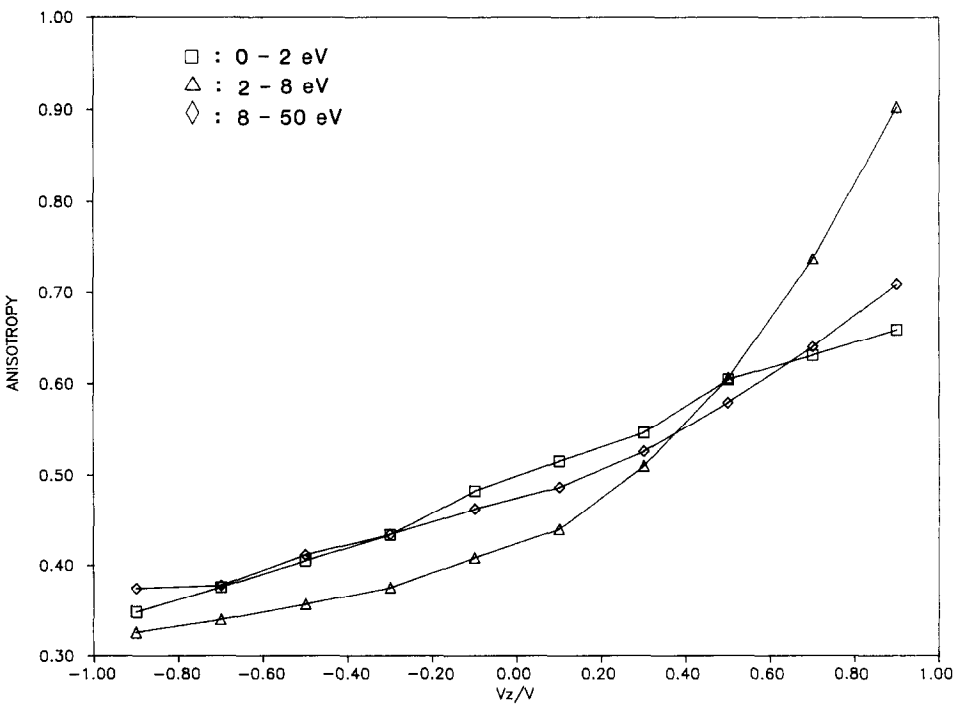

FIG. 7. Distributions of the anisotropy $f(\mu)$ of different energy regions at $E/N = 100$ Td.

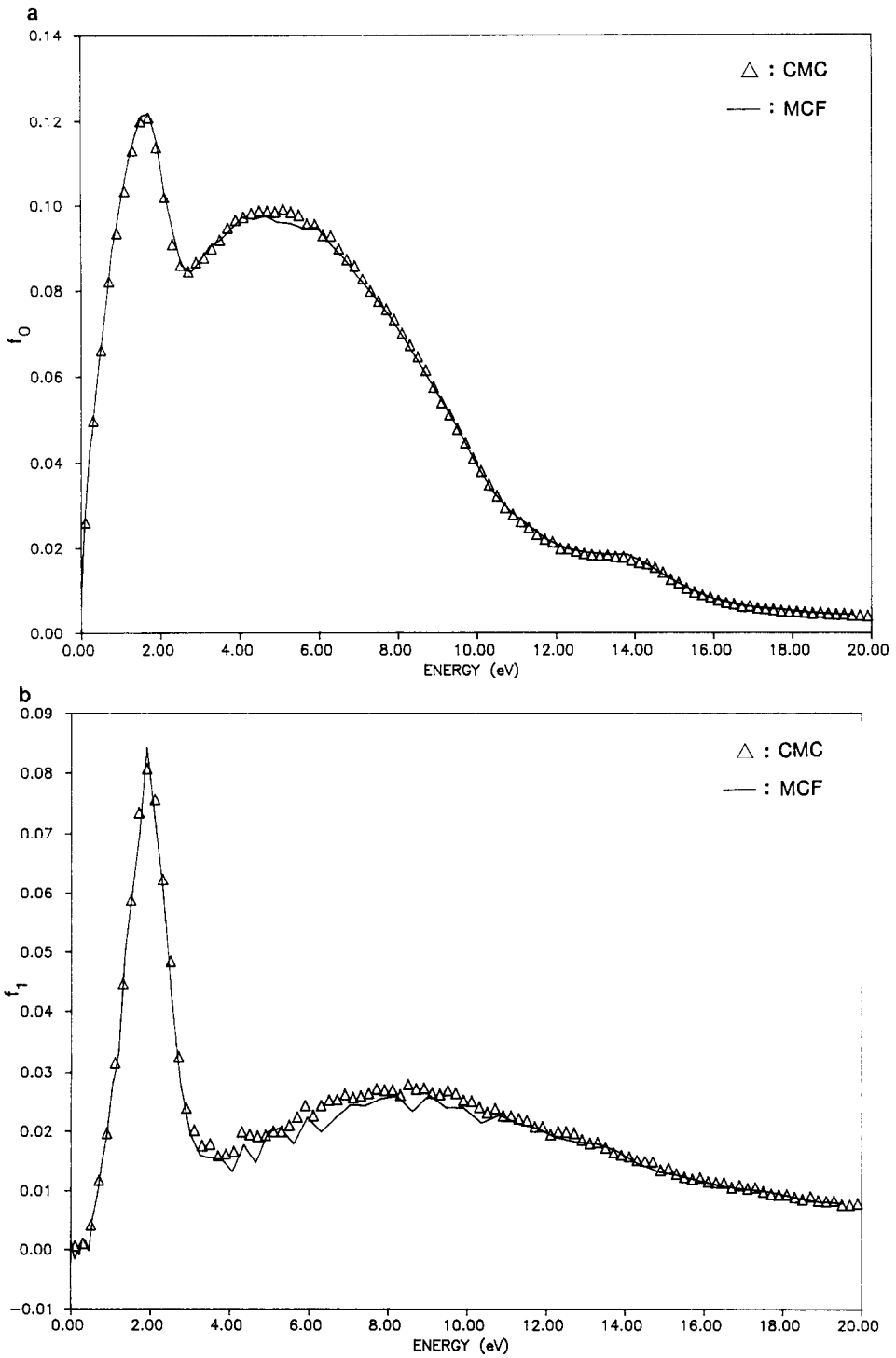

FIG. 8. The first six Legendre coefficients of the energy distribution function in N_2 at $E/N = 300$ Td: (a) $f_0(\varepsilon)$; (b) $f_1(\varepsilon)$; (c) $f_2(\varepsilon)$; (d) $f_3(\varepsilon)$; (e) $f_4(\varepsilon)$; (f) $f_5(\varepsilon)$.

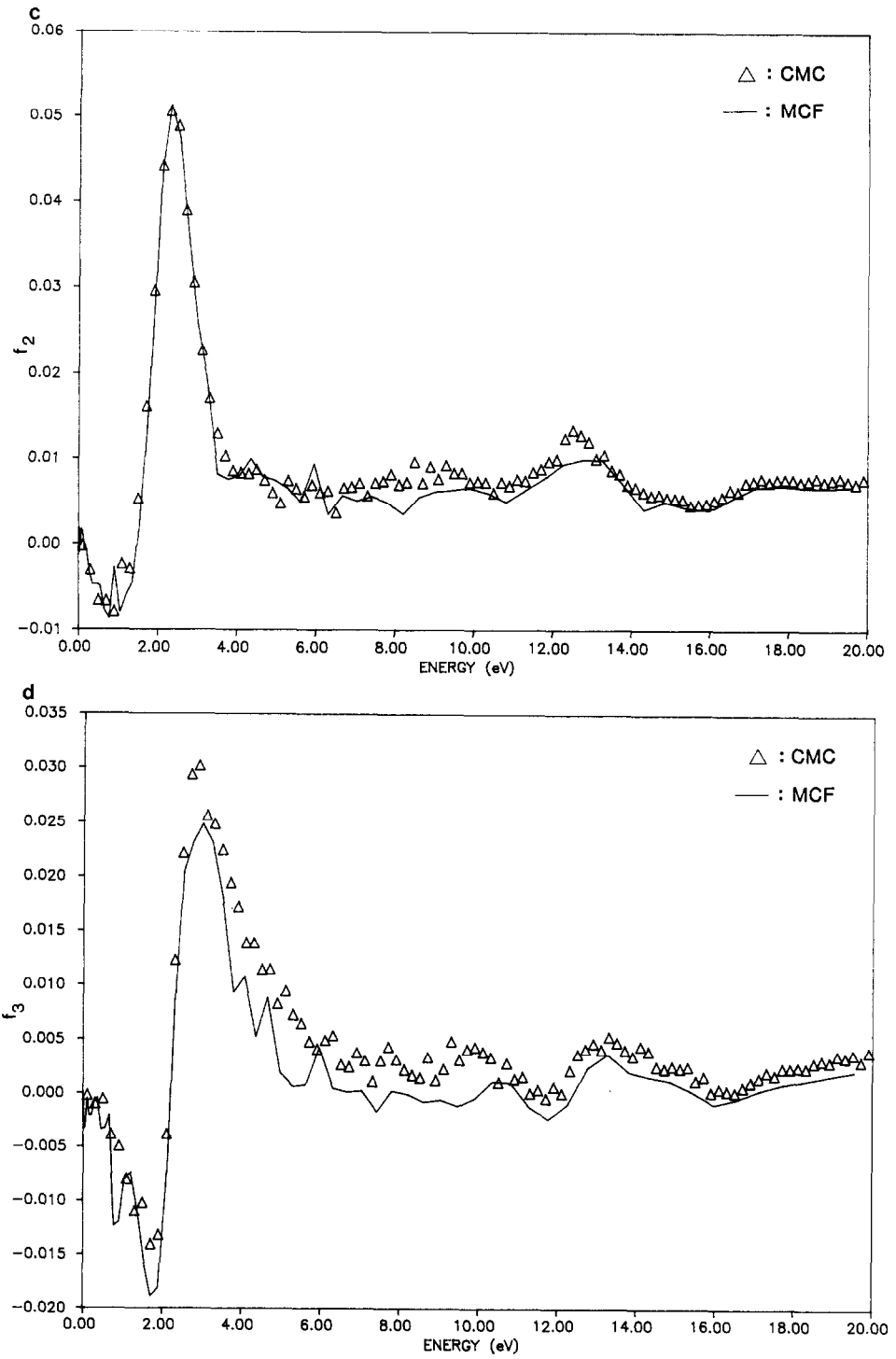

FIGURE 8 (*continued*)

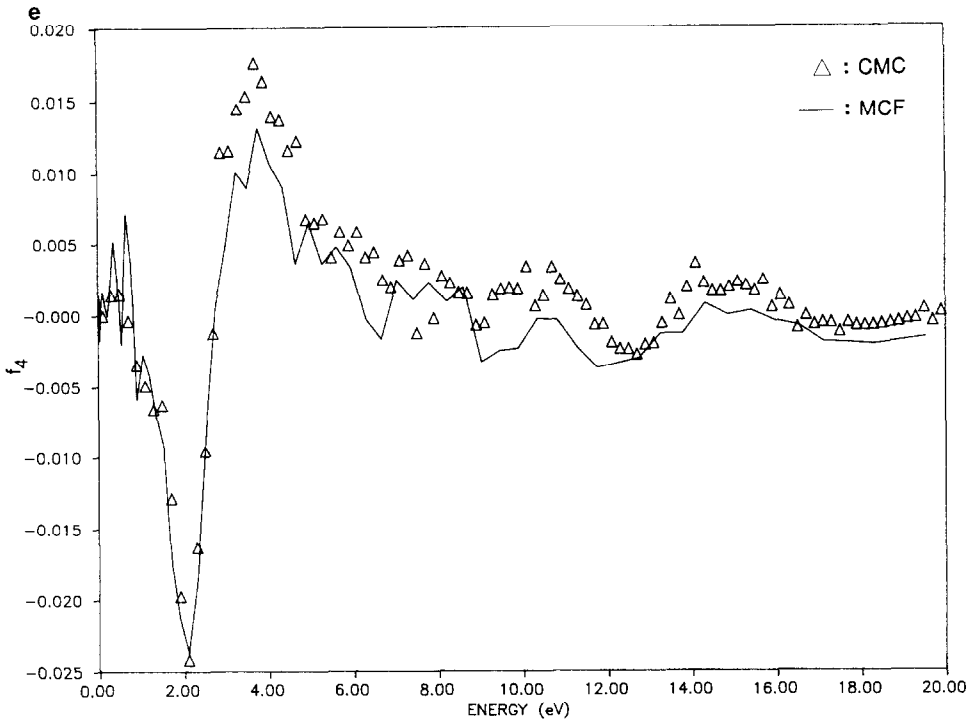

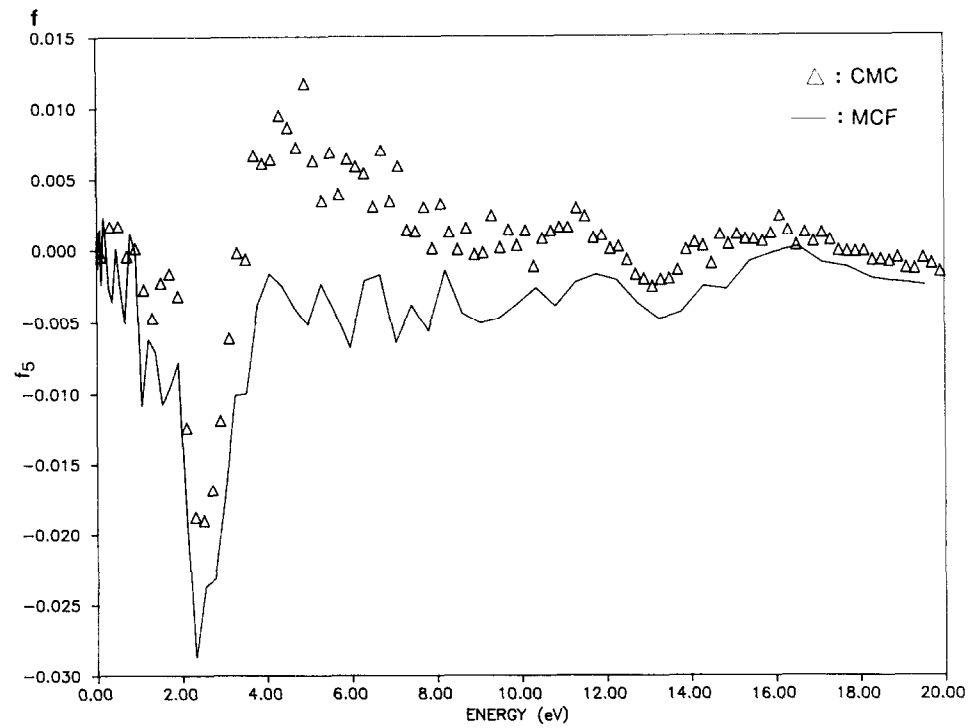

FIGURE 8 (*continued*)

MCF method are plotted in Fig. 9 to demonstrate the importance of high order moments at this value of E/N. We assume that, especially for high energies, the data obtained with the MCF method are more reliable since the resolution of the CMC method is limited in the wings of the distribution.

At this time we did not compare the Legendre coefficients calculated with the MCF method with those evaluated with a multiterm Boltzmann analysis. Such comparison is available for the CMC method [17].

3. *Transient Electron Distribution Functions*

The equation used to calculate transient distribution functions is the transport equation (7). The same transition matrix used to calculate the steady state distribution function can also be used to calculate the time dependent development of the distribution function at a given value of the reduced electric field E/N for any initial condition. Figures 10 and 11 show, as examples, the time dependence of the energy distribution, $f(\varepsilon, t)$, and anisotropy, $f(\mu, t)$, after an E/N step from 100 to 300 Td.

A similar calculation with a CMC code would be extremely time-consuming. We, therefore, performed CMC calculations with only 10^5 electrons. Thus, the distribution function shows significant fluctuations. For comparison we used the

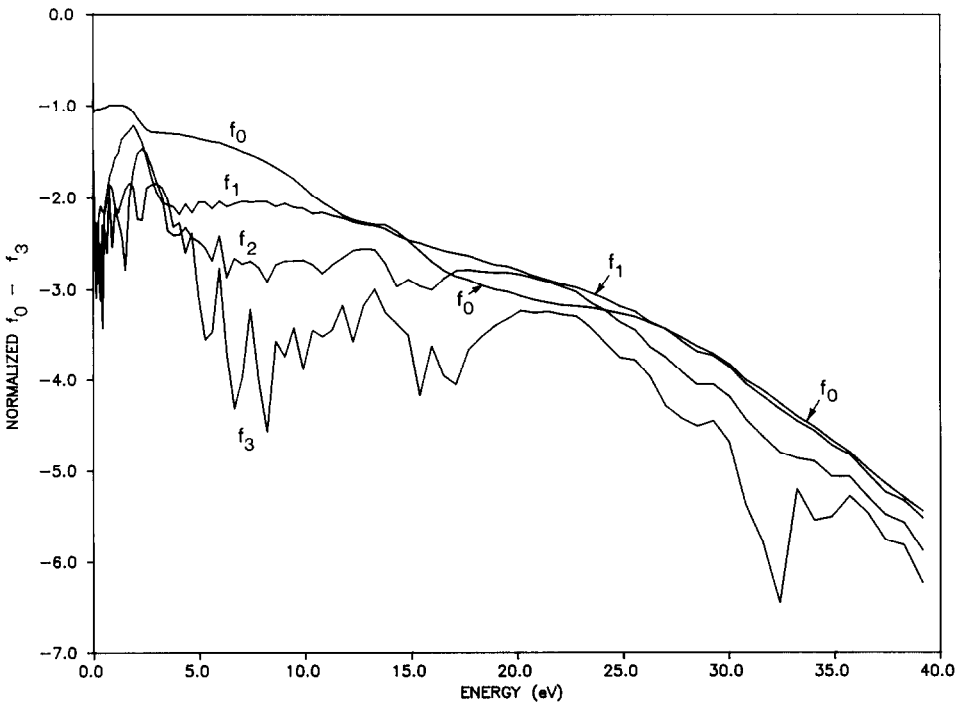

FIG. 9. The first four normalized Legendre coefficients of the distribution function in N_2 at $E/N = 300$ Td obtained using the MCF method (in logarithmic scale).

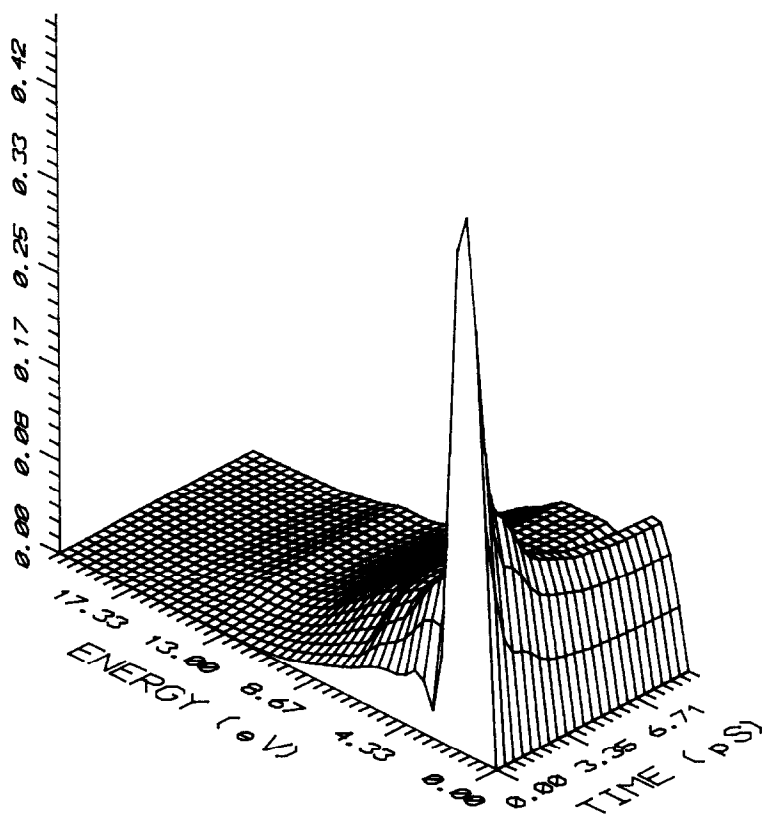

FIG. 10. Relaxation of the electron energy distribution function with time after an E/N step from 100 to 300 Td in N_2.

time-dependence of the mean energy and the drift velocity, as shown in Figs. 12 and 13 for E/N steps from 100 to 300 Td and vice versa. These curves show good agreement between the results obtained with the two different methods. The drift velocity calculated with the CMC method, however, shows strong fluctuations because of the limited number of electrons followed.

Figure 12 shows the difference between the energy relaxation times for the step up (~ 10 ps) and for the step down (~ 35 ps). Figure 13 shows the initial faster response of the drift velocity to the changes of E/N leading to an overshoot and, for the E/N step up, even to an oscillation of the drift velocity. The steady state values are reached at times similar to the relaxation times for the mean energy. However, at low values of E/N the time for the drift velocity to reach steady state is much smaller than the one for the mean energy.

It should be mentioned that the scaling quantity for relaxation phenomena at constant values of E/N is the product of time, t, and density of background gas, N,

as long as the discharge characteristic is dominated by two body collisions with neutrals. The relaxation phenomena shown in Figs. 12 and 13 should, therefore, be accessible to experimental investigations in discharges at low pressure.

4. *Incorporation of Ionization and Recombination Processes*

To illustrate how easily the MCF method can deal with electron generation and depletion processes we calculated the distribution functions and electron densities for both steady state and transient cases with the ionization and recombination processes occurring at the same time. The recombination process considered here was dissociative recombination of electrons with N_4^+ ions [18]. After obtaining the two matrices $\mathbf{P}_1(t_s)$ and $\mathbf{P}_2(t_s)$ (see Section III.5), the steady state electron density was calculated by using Eq. (10). Then the distribution function was evaluated using Eq. (9). Figure 14 presents the distribution functions at $E/N = 300$ Td, for the two cases, with and without ionization and recombination. It can be seen that in the energy range from 0 to 6 eV the electron energy distribution function with ionization and recombination is higher than the one without these processes. Above

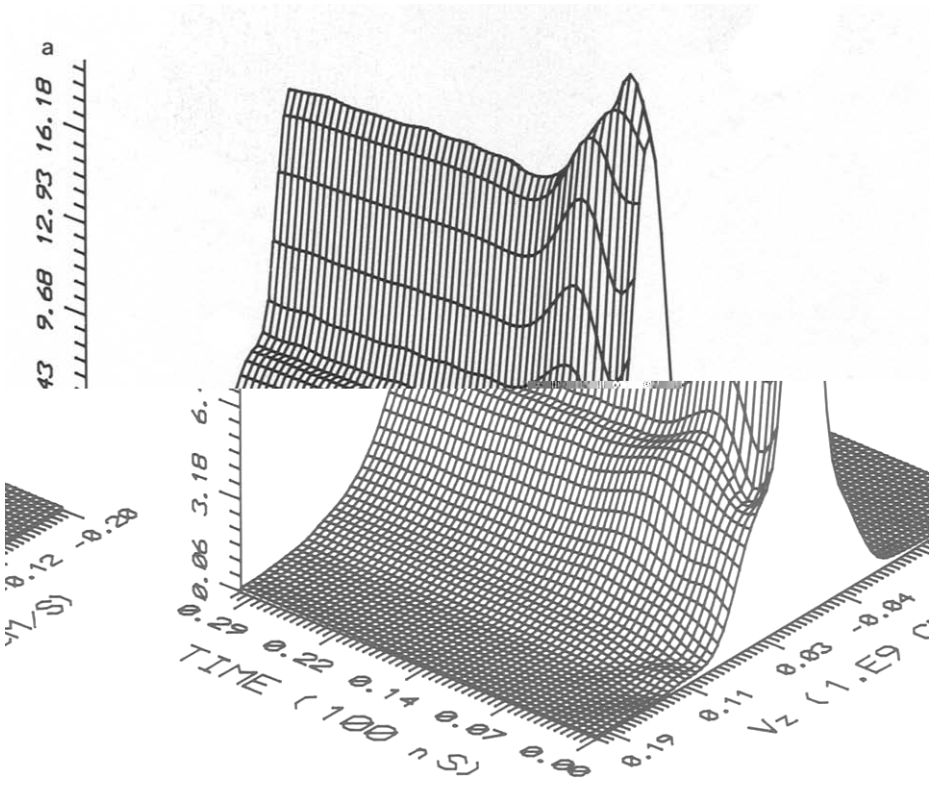

FIG. 11. Relaxation of the distribution function of the velocity in field direction, v_z, with time after an E/N step from 100 to 300 Td in N_2, looking at the: (a) positive v_z direction; (b) negative v_z direction.

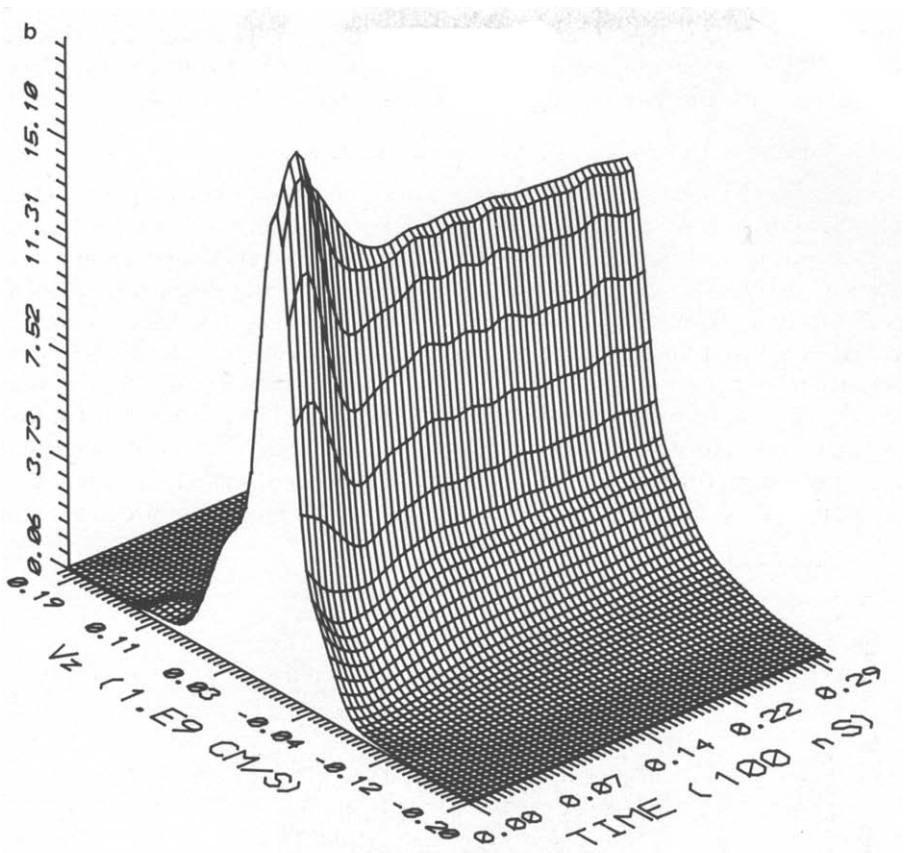

FIGURE 11 (*continued*)

6 eV it is the other way around. The major reasons are that a fast electron is needed for ionization and that the primary and secondary electrons, as a result of ionization, appear in the low energy range.

For the transient case both the initial distribution and the electron density were updated by using the transport equation (7) in which the transition matrix, $\mathbf{P}(t_s)$, is defined by Eq. (19). The relaxations of mean energy and drift velocity are quite similar to the ones shown in Figs. 12 and 13 for the case without ionization and recombination. The evolution of the electron density with time for E/N steps up and down are shown in Fig. 14. For the case of an E/N step up, from 100 to 300 Td, the time constant for the electron density is much larger than the one for the mean energy or even the drift velocity. Within the first 0.4 ns, ionization dominates and the electron density increases exponentially. Then, at higher electron densities, recombination starts to play a role in the relaxation process and the growth rate of the charged particles is reduced. Steady state is reached in

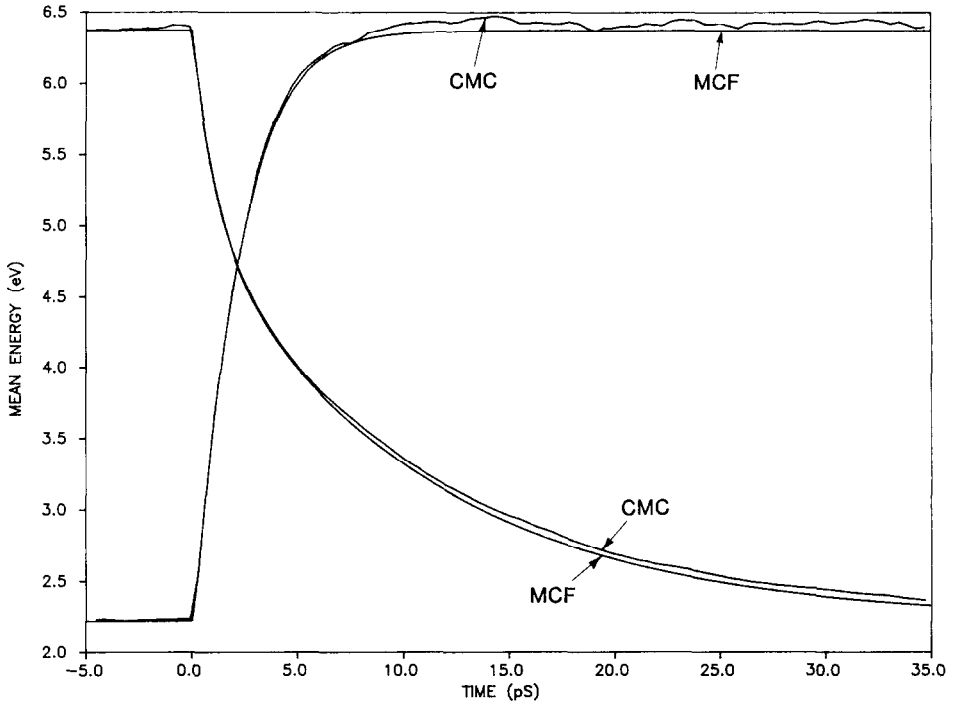

FIG. 12. Relaxation of the mean energy for E/N steps from 100 to 300 Td and vice versa.

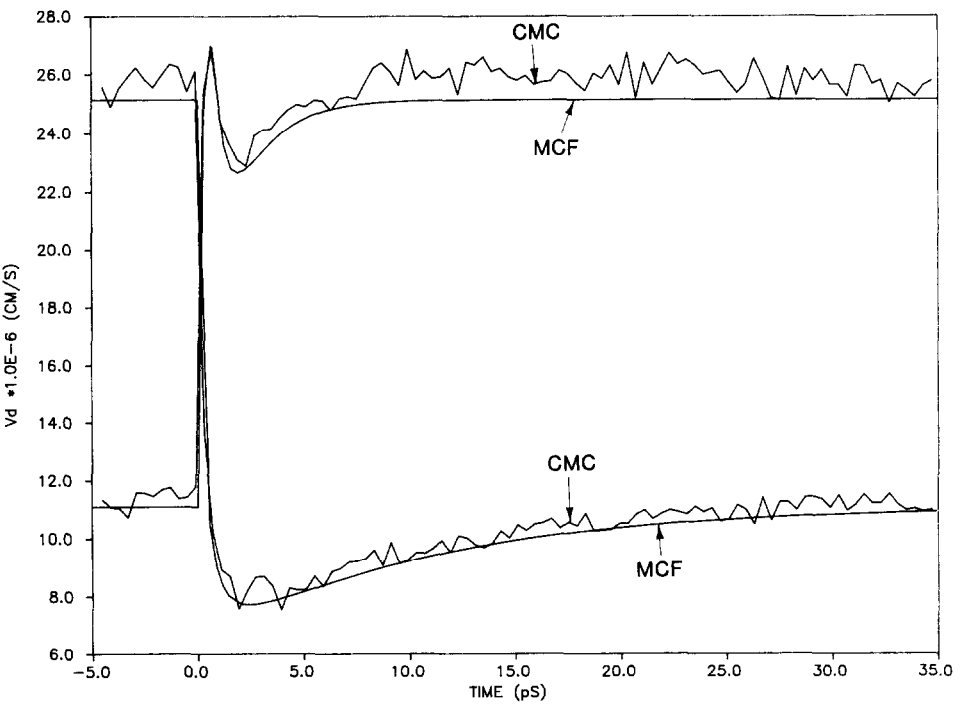

FIG. 13. Relaxation of the drift velocity for E/N steps from 100 to 300 Td and vice versa.

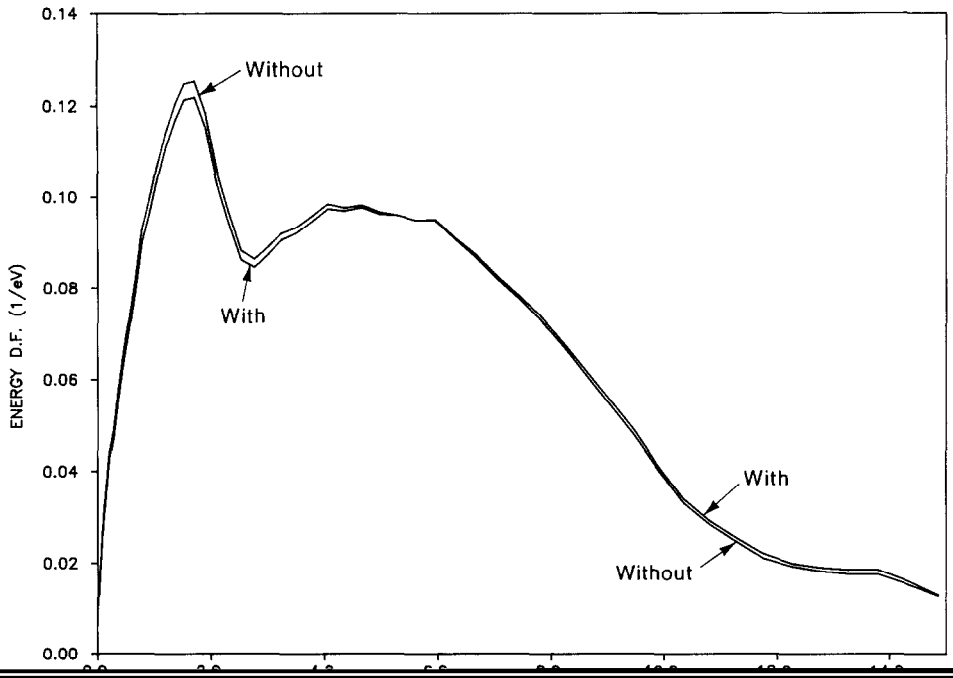

nation at $E/N = 300$ Td.

approximately 1 ns. For the case of an E/N step down, the relaxation time for the electron density is much larger than the relaxation times of drift velocity and mean energy, since it is dominated by recombination at lower electron densities. It takes a long time for the electron density to reach steady state, as shown in Fig. 14.

If we use the original transition matrix with the sampling time, t_s, to update the electron density, a very large number of numerical iterations is required to reach steady state. This problem can be solved by using the transition matrix $\mathbf{P}_m(mt_s)$, defined in Eq. (25), describing time steps of mt_s.

5. *Comparison of CPU Times for the Different Methods*

The code to calculate the transition matrix, $\mathbf{P}(t_s)$, for a MCF calculation and the CMC code involve essentially the same computational steps. The CPU times for both calculations are, therefore, approximately the same as long as the total number of collisions is kept constant. The MCF code for a steady state calculation requires in addition the solution of the eigenvalue equation (9); however, the CPU time for this part is only a small fraction of the CPU time required to calculate the transition matrix (< 5 %).

As discussed in Section II, the CMC method has good resolution in the energy ranges where the distribution functions are large and poor resolution in the wings

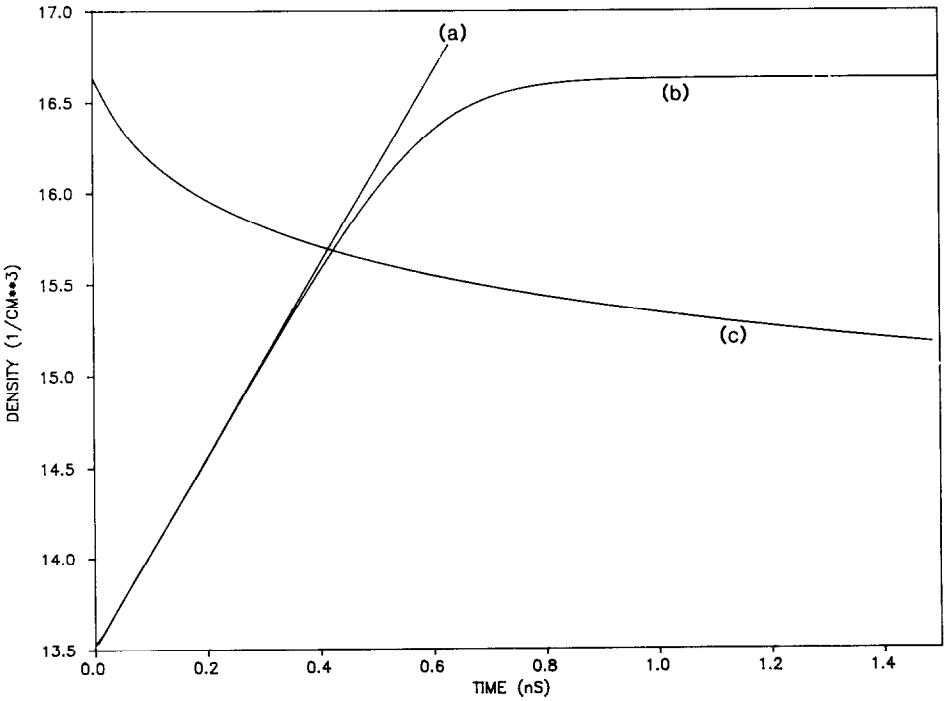

FIG. 15. Relaxation of the electron density for an E/N step from 100 to 300 Td including ionization: (a) without recombination; (b) with recombination; (c) for an E/N step from 300 to 100 Td including ionization and recombination (in logarithmic scale).

of the distributions, while the MCF method has approximately the same resolution over the full investigated range of the phase space. To improve the resolution of the CMC simulation in the wings of distribution, for example, by a factor of 10, one also has to increase the CPU time by the same factor.

The major difference in CPU time required for the two methods stems from two facts. First, the transition matrix, $\mathbf{P}(t_s)$, can also be used to calculate the time dependent development of the distribution function for any initial condition. The CPU time required to solve the transport equation (7) for a sufficiently large number of time steps (Figs. 9 to 12) was also only a small fraction of the CPU time required to calculate the transition matrix (<10 %). A similar calculation with a CMC code with similar resolution would require a CPU time at least 10^2 times higher than for the MCF method. Second, the transition matrix, $\mathbf{P}(t_s)$, is reusable for calculations with different initial conditions or different boundary conditions such as changes in the electron generation and depletion mechanisms. This means that the MCF method becomes even more efficient if a large number of calculations for different conditions are performed.

V. Conclusions

The presented calculations demonstrate the general feasibility of the MCF method in calculating electron velocity distributions for both steady state and transient cases. Major advantages are:

(1) Combination of Monte Carlo simulation and analytical methods

(2) Increase of resolution in the wings of distribution functions in any coordinate of an anisotropic distribution compared with the CMC simulation

(3) Efficiency in its application to transient distributions

(4) Easy incorporation of electron generation and depletion processes

(5) Decrease of CPU time.

All these advantages stem from the fact that a CMC code is used to calculate conditional transition probabilities, rather than population probabilities. These transition probabilities are reusable and can be used to calculate steady state and transient distribution for any initial condition.

One limitation of the MCF method is the need for a large computer memory. In our numerical calculations, the size of the transition matrix was 1000×1000 (100 intervals for the velocity and 10 for μ). However, only 20 % of all matrix elements were nonzero. The Yale Sparse Package enabled us to reduce the requirements for computer memory to at least one half. The extension of this method to fully three-dimensional distributions is, therefore, possible. The applications of the MCF method in the cases of $\mathbf{E} \times \mathbf{B}$ fields and AC and microwave discharges with different states of polarization and axial magnetic fields will be presented in a separate paper.

Acknowledgment

This work was supported by NSF Grant ECS-8711772.

References

1. W. P. Allis, "On the Divergence of the Legendre Expansion of the Electron Velocity Distribution," in *Electrical Breakdown and Discharges in Gases*, edited by E. E. Kunhardt and L. H. Luessen (Plenum, New York, 1983), Vol. 89a, p. 187.
2. L. E. Kline and J. G. Siambis, *Phys. Rev. A* **5**, 794 (1972).
3. E. E. Kunhardt and Y. Tzeng, *J. Comput. Phys.* **67**, 279 (1986).
4. Y. M. Li and L. C. Pitchford, *Appl. Phys. Lett.* **54**, No. 15, 1403 (1989).
5. G. Schaefer, G. F. Reinking, and K. H. Schoenbach, *J. Appl. Phys.* **61**, 120 (1987).
6. A. Philips and P. J. Price, *Appl. Phys. Lett.* **30**, 528 (1977).
7. M. Cheng and E. E. Kunhardt, *J. Appl. Phys.* **63**, 2322 (1988).
8. G. Schaefer and P. Hui, "The Monte Carlo Flux Method," POLY-WRI-1518-87, 1987 (unpublished).
9. P. Hui and G. Schaefer, 40th Annual Gaseous Electronic Conference, MB-4, Atlanta, October 1987.

10. G. SCHAEFER AND P. HUI, 41st Annual Gaseous Electronics Conference, KA-2, Minneapolis, October 1988.
11. S. D. ROCKWOOD, *Phys. Rev. A* **8**, 2348 (1973).
12. F. R. GANTMACHER, *The Theory of Matrices* (Chelsea, New York, 1977), Vol. 2, p. 82.
13. C. B. OPAL, W. K. PETERSON, AND E. C. BEATY, *J. Chem. Phys.* **55**, 4100 (1971).
14. Y. TZENG AND E. E. KUNHARDT, *Phys. Rev. A* **34**, 2148 (1986).
15. S. YOSHIDA, A. V. PHELPS, AND L. C. PITCHFORD, *Phys. Rev. A* **27**, 2858 (1983).
16. A. V. PHELPS AND L. C. PITCHFORD, JILA Information Center Report No. 26, 1985 (unpublished).
17. L. C. PITCHFORD AND A. V. PHELPS, *Phys. Rev. A* **25**, 540 (1982).
18. M. WHITAKER, M. A. BIONDI, AND R. JOHNSON, *Phy. Rev. A* **24**, 743 (1981).